# Single molecule analysis of the self-assembly process operated by host-guest interactions

Fu-Na Meng‡, Xuyang Yao‡, Yi-Lun Ying*, Junji Zhang, He Tian, Yi-Tao Long*

Key Laboratory for Advanced Materials & Department of Chemistry, East China University of Science and Technology, 130 Meilong Road, Shanghai, 200237, P.R. China.

Email: ytlong@ecust.edu.cn;yilunying@gmail.com

‡These authors contributed equally to this work.

## Supplementary Information

### 1. Materials.

a-Hemolysin (a-HL) wildtype-D8H6 was produced by expression in BL21 (DE3) pLysS *Escherichia coli* cells and self-assembled into heptamers. 1,2-diphytanoly-*sn*-glycero-3-phosphocholine (chloroform, ≥99%) was purchased from Avanti Polar Lipids Inc (AP, Shanghai, China). Decane was purchased from Sigma-Aldrich (≥ 99%, St. Louis, MO, USA). All the other chemicals were of analytical grade unless otherwise indicated. All solutions for analytical studies were prepared with ultrapure water (reach a resistivity of 18.2 MΩ·cm at 25 °C) obtained by the Milli-Q System (EMD Millipore, Billerica, MA, U.S.A.). The ultrapure water used in RNA preparing was treated with DEPC.

### 2. Protein Preparation

a-Hemolysin (a-HL) wild type-D8H6 was produced by expression in BL21 (DE3) pLysS *Escherichia coli* cells, and then purified by Ni column.[1] The monomer and heptamer proteins were separated by 8% SDS-PAGE. The heptamer band was cut from the gel. The purified heptamer was conserved in 10 mM Tris-HCL, 1 mM EDTA, pH 8.0 buffer and stored at -80 ℃.

### 3. Formation of the *a*-HL nanopore and electrical recording

The lipid bilayers were created by applying diphytanoyl phosphatidylcholine (30 mg/mL) in decane (≥99%, Sigma-Aldrich, St. Louis, MO, USA) to a 50 μm orifice in a 1 mL bilayer chamber (Warner Instruments, Hamden, CT, USA) filled with KCl (1.0 M) and Tris-HCl (10 mM, pH = 8.0).[2] A bilayer was deemed stably by monitoring its resistance and capacitance. The two compartments of the bilayer chamber are termed *cis* and *trans*, where the *cis* compartment is defined as virtual ground. Thus, a negative potential indicates a higher potential in the *cis* chamber. The potential was applied at -60 mV by an Ag/AgCl electrode. The experiments were run under voltage-clamp conditions using a patch clamp amplifier (Axopatch 200B; Axon instruments, Foster City, CA, USA). The amplifier's internal low-pass Bessel filter was set as 5 kHz. Data were required at a sampling rate of 100 kHz by using a DigiData 1440A converter and a PC running PClamp 10.2 (Axon Instruments, Forest City, CA, USA).

The α-HL was injected adjacent to the aperture in the *cis* chamber, and meanwhile the potential was applied +100 mV from the *cis* side to promote α-HL insertion. The pore insertion was determined by a well-defined jump in current value. Once a stable single pore insertion was detected, the analyte was added to the *trans* chamber and the potential was then changed to -60 mV. The mixtures of [MV$^{2+}$]/[SC6] were obtained by preincubating SC6 and MV$^{2+}$ for more than 20 min at room temperature before being added into the *trans* chamber.

### 4. Data analysis

Data analysis was performed using home-designed software and OriginLab 8.0 (OriginLab Corporation, Northampton, MA, USA). The blockage events with blockage current larger than a threshold value of 7 pA were recorded and analyzed. The current blockages are described as $I/I_0$, where $I_0$ is the ionic current for the empty nanopore and $I$ is the blockage current for the analyte partitioning into the nanopore. The values of I and $I_0$ were

obtained by the fitted Gaussian distributions. Data analysis was performed using home-designed software Nanopore Analysis (http://people.bath.ac.uk/yl505/nanoporeanalysis.html) and OriginLab 8.0 (OriginLab Corporation, Northampton, MA, USA). Data of the errors were based on three separate experiments. The exponential functions used to fit event frequencies of Distribution I and Distribution II in Fig. 3c are the eq.1 and eq. 2 as follows:

$$y = y_0 - A_1 e^{-(x-x_0)/t_1} - A_2 e^{-(x-x_0)/t_2} \qquad \text{eq.1}$$
$$y = y_0 - A_1 e^{(x-x_0)/t_1} - A_2 e^{(x-x_0)/t_2} \qquad \text{eq.2}$$

## 5. Nanopore analysis of *para*-sulfonatocalix[6]arenes (SC6) and methyl viologen (MV$^{2+}$)
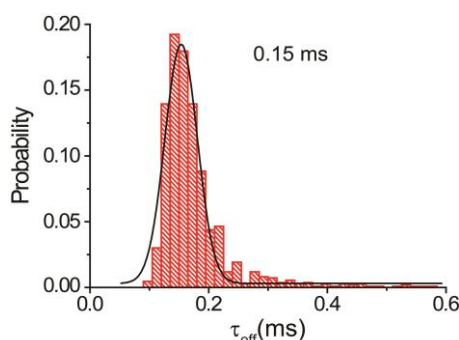


**Fig. S1** The histogram for $\tau_{off}$ of 150 μM SC6 induced blockages from *trans* side of *a*-HL at -60 mV. The histogram of $\tau_{off}$ was fitted by Gaussian function and the fitted value is 0.15 ms. Experiments were carried out in the chambers containing 1.0 M KCl buffered with 10 mM Tris-HCl (pH=8.0).
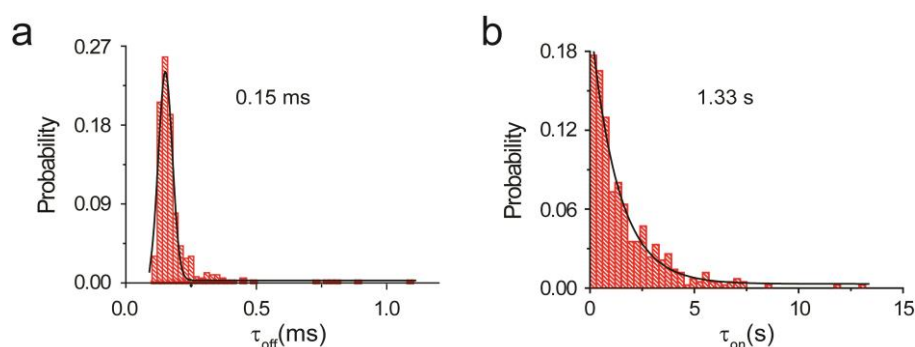


**Fig. S2** The duration time $\tau_{off}$ (a) and the event-intervals $\tau_{on}$ (b) distribution of the blockages induced by 200 μM SC6 in the *trans* side of *a*-HL at -100 mV. The histogram of $\tau_{off}$ was fitted by Gaussian function and that of $\tau_{on}$ were fitted by single exponential function. Experiments were carried out in the chambers containing 1.0 M KCl buffered with 10 mM Tris-HCl (pH=8.0).
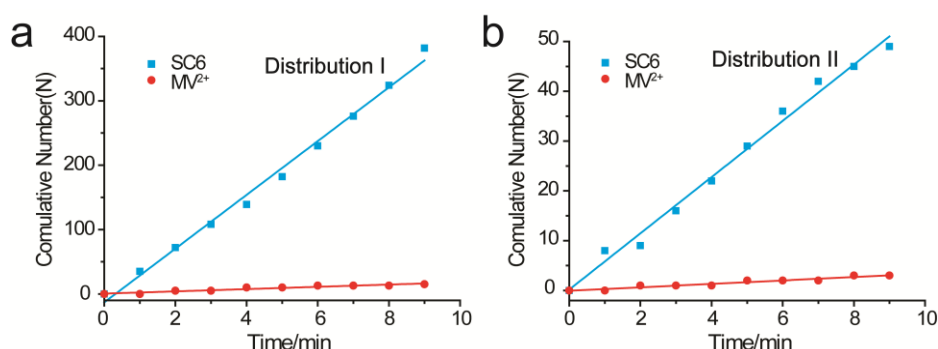


**Fig. S3** The number of cumulative event numbers versus detection time for the blockages of SC6 (blue) and MV$^{2+}$ (red) distributed in Distribution I (a) and Distribution II (b), respectively. The final concentration SC6 and MV$^{2+}$ in the *trans* chamber were 150 μM and 800 μM, respectively. The slops represent the event frequencies. SC6 produced the event frequencies of 47.6 ± 5.2 and 5.1 ± 1.2 events/min for the blockages in Distribution I and Distribution II, respectively. The blockages of MV$^{2+}$ generated the event frequencies of 1.8 ±0.5 and 0.3 ±0.1 events/min, respectively. Experiments were carried out in the chambers containing 1.0 M KCl buffered with 10 mM Tris-HCl (pH=8.0) at potential of -60 mV.

## 6. Translocation mechanisms of 1:1 and 1:2 complex through an $\alpha$-HL nanopore

As shown in Fig. S4, the value of $\tau_{off}$ for 1:1 complex is about 0.16 $\pm$0.01 ms, which is comparable to that for SC6 alone (0.15 $\pm$0.01 ms). SC6 adopts cone conformation as it forms binary complexes (Fig. 1).[3-4] The diameter of SC6 in cone conformation is about 0.7 nm while $\alpha$-HL has a constriction part of d $\approx$ 1.4 nm. Therefore, 1:1 complex either traverses through $\alpha$-HL or bumps against the *trans*-side opening of the pore to generate the short-lived blockages. The addition of 1:2 complex induced a Distribution II of long-lived blockages with large amplitudes. As shown in Fig. 2c-f and Fig. S4, the $\tau_{off}$ of the long-lived blockages in Distribution II is about 0.28 $\pm$ 0.02 ms, which is larger than that of short-lived blockages in Distribution I generated by 1:1 complex (0.16 $\pm$0.01 ms). Meanwhile, the peak current of Distribution II has a larger value of $I/I_0$=0.73 $\pm$0.02 than that of Distribution I which is 0.25 $\pm$0.02. As discussed in previous studies, 1:2 complex adopts the 1,2,3-alternate conformation as it forms ternary complex (Fig.1).[5-6] On account of the large volume, 1:2 complex blocked the majority of the ionic current through the $a$-HL, leading to the blockages in Distribution II. Therefore, the volume exclusion is the major factor which affects the translocation mechanism of 1:1 and 1:2 complex.

**Table S1** The event frequencies for blockages located in Distribution I and Distribution II at different ratio of $[MV^{2+}]/[SC6]$. The ratio of $[MV^{2+}]/[SC6]$ ranged from 0.2 to 5 in the *trans* chamber at -60 mV. The concentrations of SC6 in the mixtures were kept at 150 $\mu$M.

| $[MV^{2+}]/[SC6]$ | Event Frequency (events/min) | |
| --- | --- | --- |
| | Distribution I | Distribution II |
| 0.2 | 94.1 $\pm$14.1 | 5.3 $\pm$0.6 |
| 0.5 | 81.5 $\pm$11.4 | 8.3 $\pm$1.2 |
| 1 | 78.6 $\pm$10.2 | 11.6 $\pm$1.5 |
| 1.5 | 71.1 $\pm$10.7 | 16.1 $\pm$1.9 |
| 2 | 64.7 $\pm$7.8 | 16.6 $\pm$2.0 |
| 2.5 | 63.0 $\pm$8.2 | 20.2 $\pm$2.2 |
| 3.5 | 56.7 $\pm$8.5 | 19.7 $\pm$3.0 |
| 5 | 54.8 $\pm$6.6 | 24.6 $\pm$2.5 |



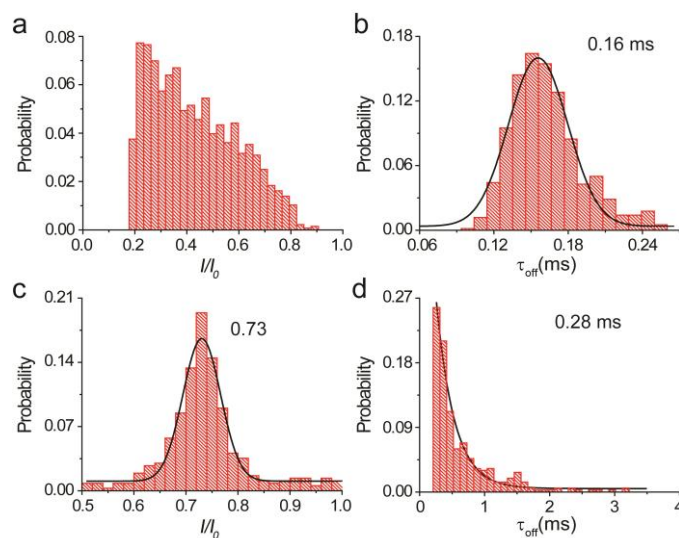**Fig. S4** The histograms of blockage current and the duration time for the blockages in Distribution I at $[MV^{2+}]/[SC6] = 0.2$ (a, b) and the blockages in Distribution II at $[MV^{2+}]/[SC6] = 5$ (c, d). SC6 were fixed at 150 $\mu$M in *trans* chamber which contains 1.0 M KCl buffered with 10 mM Tris-HCl (pH=8.0) at potential of -60 mV. The histograms of $\tau_{off}$ for Distribution I (b) and blockage current $I/I_0$ for Distribution II (c) were fitted by Gaussian function. Single exponential function was used to fit the histograms of $\tau_{on}$ for Distribution II.
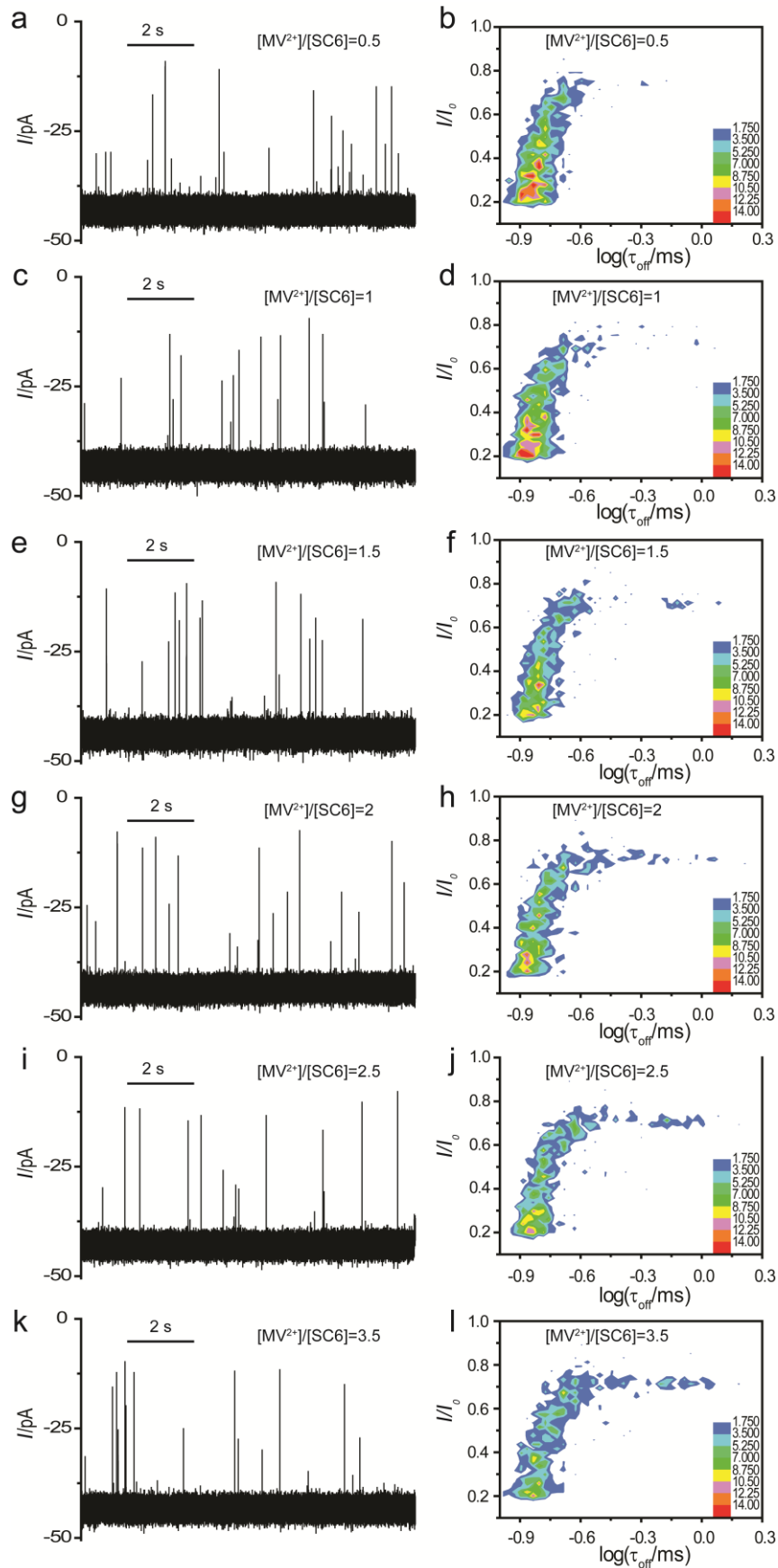
**Fig. S5** The raw data and 2D counter plots for the blockages generated by the mixture of $[MV^{2+}]/[SC6]= 0.5$ (a, b), 1 (c, d), 1.5 (e, f), 2 (g, h), 2.5 (i, j) and 3.5 (k, l). The blockages used in the 2D counter plots obtained by continuous recording for 14 min during the nanopore experiments. The current traces were recorded in solutions containing 1.0 M KCl buffered with 10 mM Tris-HCl (pH=8.0) at -60 mV. The concentrations of SC6 in the mixtures were kept at 150 μM.

The frequencies of Distribution II exponentially increased as the ratio of $[MV^{2+}]/[SC6]$ increased gradually from 0.2 to 5. Besides 1:2 complex, SC6 also contributed to the blockages in Distribution II (Fig. S3). Since the increase amount of $[MV^{2+}]$ poises the self-assembly process in favor of 1:2 complex, we hypothesize that the contribution of SC6 to the frequency of Distribution II has a contrary trend with changes of $[MV^{2+}]/[SC6]$. Assuming that the absolute value of the decay constant for the contribution of SC6 to the frequency of blockages in Distribution II was the same as the increase constant of the blockages frequency of Distribution II, we could estimate the contributions of SC6 to the frequency of blockages in Distribution II in all mixtures. The eq. 2 was used to fit the trend of frequency in Distribution II. Thus, the contributions of SC6 to the frequency of Distribution II decreased exponentially from 5.1 to 0.0 events/min as the ratio of $[MV^{2+}]/[SC6]$ increased from 0.0 to 0.5 (Fig. S6).When $[MV^{2+}]/[SC6] > 0.5$, the frequencies of Distribution II could be entirely attributed to the 1:2 complex. Then, the contributions of SC6 could be eliminated from the frequencies of Distribution II (Fig. S6). As calculated by eq. 2, the exponential fitting shows that the saturated frequency of Distribution II ($y_0$) is 26.4 events/min which corresponds to the maximum concentration of 1:2 complex (150 μM). As shown in Fig. 3d, the concentrations of 1:2 complex in the mixture could be calculated based on the amended frequencies of Distribution II.
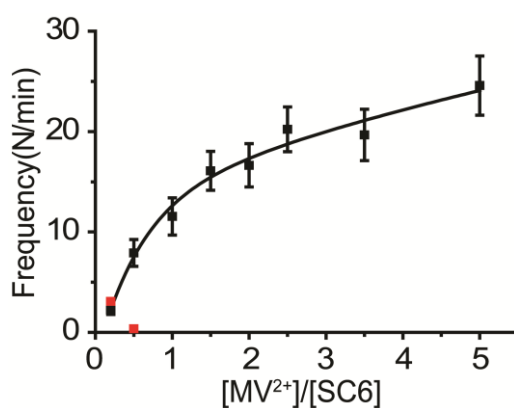


**Fig. S6** The contributed blockage frequency of SC6 to Distribution II (red) and the frequency of Distribution II ascribed to 1:2 complex after the contribution of SC6 was eliminated (black).

### 7. Binding behavior between SC6 and MV$^{2+}$

The information of self-assembled complex between host molecules SC6 and guest molecules MV$^{2+}$ is evident in $^1H$ NMR spectroscopic experiment in D$_2$O (Fig. S7-S8). In the presence of SC6, the protons of MV$^{2+}$-CH$_3$ (marked with red star in Fig. S7) exhibit a visible upfield shift due to the ring current effect of the aromatic nuclei, which suggests that the MV$^{2+}$ is encapsulated into the cavity of SC6. However, the protons of the aromatic protons of SC6 changed from one singlet to two singlets as the ratio of $[MV^{2+}]/[SC6]$ increased from 1 to 2, which indicated the formation of 1:2 complex (Fig. S9). [7]
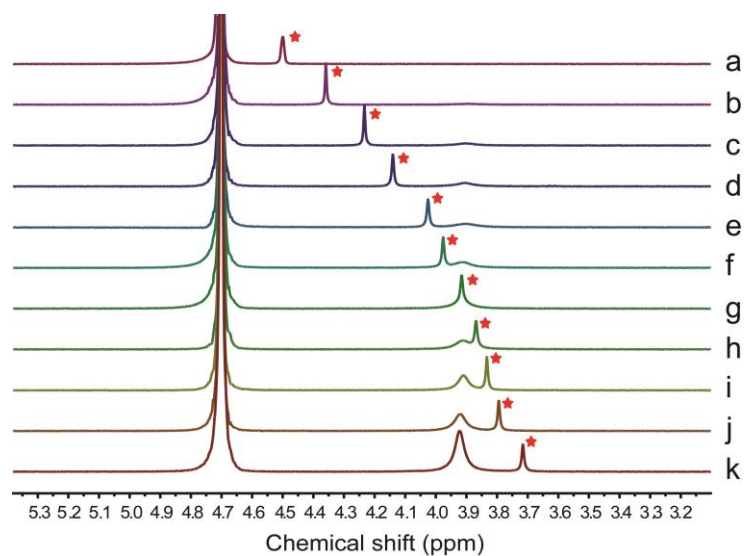
**Fig. S7** $^1$H NMR spectrum (400 MHz, 298 K) of $MV^{2+}$-$CH_3$ (marked with red star) in 1 M KCl $D_2O$ solution at the ratio of $[SC6]/[MV^{2+}]$ = 0 (a), 0.14 (b), 0.28 (c), 0.42 (d), 0.64 (e), 0.70 (f), 0.84 (g), 0.98 (h), 1.12 (i), 1.40 (j), 2.80 (k). The concentration of $MV^{2+}$ is 1 mM at $[SC6]/[MV^{2+}]$=0 while that of $MV^{2+}$ is 2 mM at $[SC6]/[MV^{2+}]$ from 0.14 to 2.80. The unmarked peak refers to the protons on methylene of SC6.



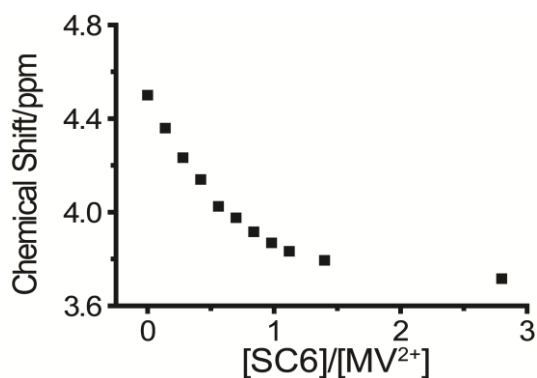**Fig. S8** Dependence of the chemical shifts of $MV^{2+}$-CH3 protons at the ratio of $[SC6]/[MV^{2+}]$ ranging from 0 to 2.80. The concentration of $MV^{2+}$ is fixed at 2 mM.



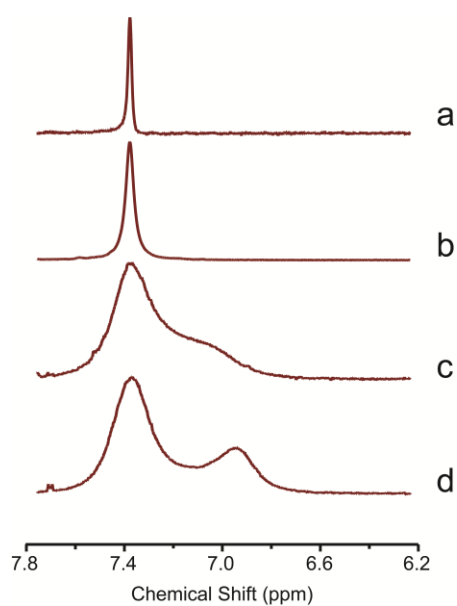**Fig. S9** $^1$H NMR spectrum (400 MHz, 298 K) for the aromatic protons of SC6 at $[MV^{2+}]/[SC6]$= 0 (a), 1 (b), 2 (c) and 5 (d) in 1 M KCl $D_2O$ solution. The intensity of the NMR peaks was not in scale.

**Reference**

1. S. Wen, T. Zeng, L. Liu, K. Zhao, Y. Zhao, X. Liu and H. C. Wu, *J. Am. Chem. Soc.*, 2011, **133**, 18312.

2. Y. L. Ying, J. Zhang, F. N. Meng, C. Cao, X. Yao, I. Willner, H.Tian and Y. T. Long, *Sci. Rep.*, 2013, **3**, 1662.

3. S. A. Fernandes, L. F. Cabeça, A. J. Marsaioli and E. de Paula, *J．Incl. Phenom. Macrocycl. Chem.*, 2007, **57**, 395.

4. Y. Sueishi, N. Inazumi and T. Hanaya, *J. Phys. Org. Chem.*, 2005,**18**, 448.

5. R. Castro, L. A. Godíñez, C. M. Criss and A. E. Kaifer, *J. Org. Chem.*, 1997, **62**, 4928.

6. N. Douteau-Guével, F. Perret, A. W. Coleman, J.-P. Morel and N. Morel-Desrosiers, *J. Chem. Soc., Perkin Trans. 2*, 2002, 524.

7. J. Alvarez, Y. Wang, W. Ong and A. E. Kaifer, *J. Supramol. Chem.*, 2001, **1**, 269.